

We are IntechOpen, the world's leading publisher of Open Access books Built by scientists, for scientists

6,900

Open access books available

186,000

International authors and editors

200M

Downloads

Our authors are among the

154

Countries delivered to

TOP 1%

most cited scientists

12.2%

Contributors from top 500 universities



WEB OF SCIENCE™

Selection of our books indexed in the Book Citation Index
in Web of Science™ Core Collection (BKCI)

Interested in publishing with us?
Contact book.department@intechopen.com

Numbers displayed above are based on latest data collected.
For more information visit www.intechopen.com



Calcium Uptake on Kaolinite and Gibbsite: Effects of Sulfate, pH, and Salt Concentration with Additional Insight from Second Harmonic Generation on Temperature Dependencies with Sapphire-Basal Planes and the Potential Relevance to Ice Nucleation

Ahmed Abdelmonem, Yujun Wang, Johannes Lützenkirchen and Marcelo Eduardo Alves

Abstract

Although previous studies have shown that sulfate can either increase cation leaching or enhance cation adsorption in soil, little is known about the factors behind these phenomena. To learn more about them, calcium adsorption experiments were carried out with kaolinite and gibbsite at initial pH values 4 and 6 and in the presence of 1 or 20 mmol_c L⁻¹ of either nitrate or sulfate. The results indicated that limited sulfate-calcium coadsorption occurred on gibbsite when it was in contact with the dilute solution of CaSO₄·2H₂O at pH ~ 7. Regarding mineral and pH values, calcium adsorption from the concentrated solutions decreased with sulfate possibly because of the presence of ~31% of the CaSO₄⁰ ion pair in the concentrated CaSO₄·2H₂O solutions and the low free calcium activity therein. Calcium adsorption on kaolinite and gibbsite from all concentrated solutions was reduced when the initial pH changed from 4 to 6 suggesting a negative salt effect on that process. In addition to indicating negligible participation of gibbsite in calcium adsorption, our findings also suggest that higher amounts of gypsum applied to lime-amended oxisols reduce the effectiveness of the main oxisol clay-sized mineral capable of adsorbing cations, i.e., kaolinite, to impair calcium leaching. The uptake data were complemented with some zeta-potential measurements, which supported the lack of substantial uptake of calcium even in the presence of sulfate. Some modeling calculations using the only available model covering sulfate and calcium on gibbsite have been done to rationalize the experimental data, but the model is only able to involve pure electrostatic attraction of calcium, which is not sufficient to produce

substantial uptake. Finally, the aluminol basal plane that is present on both gibbsite and kaolinite has been additionally studied using second harmonic generation (SHG) down to 4°C, because the ion-pair formation decreases with decreasing temperature. The second harmonic results confirm the patterns observed in the electrokinetic measurements with kaolinite being quite comparable to the sapphire basal plane. Also and quite clearly, the presence of CaSO₄ solutions caused temperature dependence different from pure CaCl₂ and Na₂SO₄ solutions. The latter were essentially behaving like pure water. The difference between the calcium chloride and sulfate systems can be explained by sulfate interaction and might be linked to the temperature dependence of the formation of the CaSO₄ ion pair. The temperature dependency study could be an important starting point for looking at ice nucleation in the presence of the three different solutions and more strongly link aqueous chemistry to ice nucleation processes.

Keywords: acidic soils, double-layer screening, gypsum, leaching, oxisols, ice nucleation

1. Introduction

Gypsum (~95% m/m CaSO₄·2H₂O) can be used as soil amendment to lessen the phytotoxicity of available aluminum found in acidic subsoil depths that, although accessible to the plant roots, are not affected by surface liming [1]. Field and laboratory experiments have indicated that gypsum application on soil can increase the leaching of plant nutrients such as potassium, calcium, and magnesium [2–5]. Such an effect could be due to the formation of negative or neutral ion pairs (e.g., KSO₄[−], CaSO₄⁰, and MgSO₄⁰) in the soil solution as predicted by the hard and soft (Lewis) acid and base theory [6]. In contrast, experiments conducted with soil samples rich in gibbsite, hematite, goethite, or allophane have suggested that sulfate adsorption enhances calcium adsorption [7–13]. Fahrenhorst et al. [4] found that the gypsum potential of increasing the cation exchange capacity (CEC) of an oxisol from Amazon corresponded on a 1:1 basis with the sulfate adsorption by that soil. Okuma and Alves [14] observed, in the absence of phosphate, that the enhancing effect of sulfate on CEC increased with the soil contents of iron and aluminum oxides. Although Pearce and Sumner [11] have suggested that the equivalent retention of Ca²⁺ and SO₄^{2−} observed in kaolinitic subsoil could be due the combination of several mechanisms, including precipitation, specific adsorption, ionic strength-induced charging, and ion-pair adsorption, to date such phenomenon remains to be clarified.

Among the surface chemical equations used to model solution pH and ionic strength effects on ion complexation on a standard gibbsite surface (≡AlOH⁰), those referring to sulfate complexation are given by [15]



The above equations indicate that sulfate adsorption to gibbsite gives rise to negatively charged surface species, decreases the net positive surface charge, and increases the solution pH. Such features could favor sulfate-cation co-adsorption even at lower pH because sulfate adsorption on gibbsite increases as pH decreases [16]. Indeed, the acidic condition is required for the formation of ternary surface complexes of copper,

lead, and cadmium with phosphate and ferrihydrite [17, 18]. Calcium complexation on gibbsite has in turn been modeled with the following equation [15]:



Although the surface chemical Eqs. (1)–(3) refer to adsorption sites located on the gibbsite edge faces, the basal planes of plate-shaped gibbsite and kaolinite as well seem to be operational in calcium adsorption as demonstrated by surface force measurements [19–21]. Considering that hydrolyzed species are preferably adsorbed to oxide surfaces [22], cations that hydrolyze at high pH values, such as calcium, would be expected not to be adsorbed on gibbsite and kaolinite edge sites at low pH. However, the above results obtained with atomic force microscopes indicate that cations presenting high hydrolysis constants can be retained on basal planes of gibbsite and kaolinite even under acidic condition.

Besides mineral surface properties, solution features must also be taken into account when evaluating ion adsorption. The formation of aqueous neutral ionic pairs can reduce the ion adsorption. The saturated solution of calcium sulfate (~15.8 mM), for instance, contains about 35% of total dissolved calcium and sulfate as the CaSO_4^0 ion-pair. Thus, both ions can be less adsorbed if such retention does not shift the equilibrium of CaSO_4^0 ion-pair formation toward the formation of free aqueous ions Ca^{2+} and SO_4^{2-} . Furthermore, even with limited aqueous ion-pair formation, an increase in the ionic strength can, in some cases, decrease ion adsorption on the solid phase [23, 24].

In this chapter, we studied the effects of the aqueous sulfate, salt concentration, and solution pH on the amounts of calcium adsorbed on kaolinite and gibbsite. These minerals were chosen because their joint contents in the oxisol clay fraction usually surpass 50% (m/m). Furthermore, while kaolinite is the most abundant cation-adsorbing mineral found in less weathered oxisols, gibbsite is the predominant clay-sized mineral in their deeply weathered counterparts [25]. The purpose of the present investigation was to evaluate the calcium adsorption behavior of kaolinite and gibbsite in oxisols amended with rich-sulfate sources such as gypsum.

2. Material and methods

2.1 Minerals

A kaolinite sample from Minas Gerais, Brazil, and a laboratory-prepared sample of gibbsite were used in the experiments. The gibbsite sample was prepared via titration of 500 mL of 1 M Al^{3+} (added as $\text{AlCl}_3 \cdot 6\text{H}_2\text{O}$) with 315 mL of 4 M NaOH followed by precipitate dialysis for 1 month against daily refreshed deionized water kept at 50°C [26]. Both samples were washed with deionized water, oven-dried (75°C/48 h), ground in an agate mortar, and passed through a 0.3-mm sieve.

The mineralogical purity of the samples was checked through powder X-ray diffraction (XRD). The XRD patterns were measured using a Philips PW1830 diffractometer (PANalytical, Almelo, the Netherlands) in continuous scan mode ($0.02^\circ 2\theta \text{ s}^{-1}$) from 3 to $90^\circ 2\theta$ $\text{CuK}\alpha$. The particle shapes were examined via scanning electron microscopy (SEM) using a LEO 435 VP microscope (LEO Electron Microscopy Inc., Thornwood, NY). The pH at the isoelectric point (IEP) was determined by graphical interpolation from zeta-potential (ζ) measurements. The ζ values were measured in triplicate with a NanoBrook Omni analyzer (Brookhaven Instruments, Holtsville, NY) in mineral suspensions (1 g L^{-1}) prepared in 0.01 M KNO_3 solutions with different pH values,

which were stabilized by additions of 0.01 M HCl or 0.01 M NaOH. The five-point N₂-BET-specific surface areas were measured in the samples with a Micromeritics ASAP 2010 surface area analyzer (Micromeritics, Norcross, GA).

2.2 Calcium adsorption experiments

Before the adsorption experiments, aqueous mineral suspensions (20 g L⁻¹) were titrated with 0.1 M HCl or 0.1 M NaOH until their pH values stabilized at 4 and 6 to mimic an unsuitable (pH 4) and a proper (pH 6) acidity condition for the most of crops. Then, the suspensions were centrifuged, and the minerals were oven-dried at 75°C for 48 h, ground in an agate mortar, and passed through a 0.3-mm sieve. Calcium solutions (0.5 and 10 mM; pH 4 and 6) were prepared from reagent-grade calcium sulfate and calcium nitrate. The above concentrations were chosen to allow for respective low and high ion pairing in the sulfate solutions. Aqueous calcium speciation (**Table 1**) was calculated using the formation constants available in the built-in database (NIST 46.7) of Visual MINTEQ [27].

Batch calcium adsorption experiments were performed without CO₂ exclusion as follows: 0.2 g of mineral and 20 mL of solution were placed into 50-mL polypropylene centrifuge tubes. The suspensions were shaken end over end at 30 rpm for 24 h at 20 ± 2°C. The pH was measured in the suspensions with a Thermo Orion 4-star pH meter (Thermo Orion Inc., Beverly, MA) after a two-point calibration with standard buffer solutions (pH 4.0 and 7.0). The tubes were centrifuged for 30 min at 10,000 rpm, and the supernatants were filtered through 0.22-μm cellulose membranes prior to calcium analysis in an atomic absorption spectrophotometer (Varian AA 240 FS, Agilent Technologies, Mulgrave, Australia). A cross-check of the initial calcium concentrations in the applied solutions was concurrent with the measurements performed in the remaining solutions. Both absolute and relative amounts of adsorbed calcium were calculated from the difference between the calcium initial and equilibrium aqueous concentrations.

Solution	pH	I ^a	Ca ²⁺	CaSO ₄ ⁰	CaNO ₃ ⁺	Ca ²⁺ ^c
		mM		% ^b		mM
0.5 mM CaSO ₄ ·2H ₂ O	4.0	02	93.3	06.7	-	0.38
0.5 mM CaSO ₄ ·2H ₂ O	6.0	02	93.2	06.2	-	0.38
0.5 mM Ca(NO ₃) ₂ ·4H ₂ O	4.0	02	99.7	-	0.3	0.42
0.5 mM Ca(NO ₃) ₂ ·4H ₂ O	6.0	02	99.7	-	0.3	0.42
10 mM CaSO ₄ ·2H ₂ O	4.0	30	69.3	30.7	-	3.68
10 mM CaSO ₄ ·2H ₂ O	6.0	30	69.2	30.8	-	3.68
10 mM Ca(NO ₃) ₂ ·4H ₂ O	4.0	30	96.8	-	3.2	5.07
10 mM Ca(NO ₃) ₂ ·4H ₂ O	6.0	30	96.8	-	3.2	5.07

^a $I = 1/2 \times \sum M_i z_i^2$, where I is the solution ionic strength calculated via Visual MINTEQ, mM; M_i and z_i are the respective concentration, mM, and charge of the dissolved specie i .
^bProportions of the main dissolved calcium species calculated via Visual MINTEQ in relation to the total calcium concentration.
^cFree calcium activity in solution calculated via Visual MINTEQ from activity coefficients assessed with the Davies equation.

Table 1.
Calcium solutions used in the sorption experiments.

2.3 Electrokinetic measurements

Electrokinetic experiments were carried out for kaolinite and gibbsite suspensions (1 g L^{-1} , pH 5) presenting increasing amounts of either calcium chloride or sodium sulfate. Additional measurements were carried out with calcium sulfate solutions including a saturated one ($\sim 15.8 \text{ mM}$) to maximize the formation of the aqueous CaSO_4^0 ion pair. The Brookhaven PALS apparatus was used. Suspensions were freshly prepared and at least 10 runs per sample were performed. These series clearly indicated the absence of time dependence, i.e., equilibration was typically on the order of 5 min.

2.4 Second harmonic generation measurements

Second harmonic generation (SHG) experiments were carried out with an alumina prism exposing the c-cut to the aqueous solution. This crystal plane is structurally equivalent to the gibbsite basal plane on both gibbsite and kaolinite. The setup has been described in detail elsewhere [28, 29]. The sapphire prism was obtained from Kyburz (Safnern, Switzerland) and cleaned based on procedures established earlier. The PTFE cell was initially cleaned as well with acetone and ethanol and copiously washed with MilliQ water. After each experimental series, the solution in the cell was replaced several times with MilliQ water until the signal obtained remained stable at the initial value of MilliQ water.

2.5 Data analysis

Uptake experiments were carried out in triplicate. The paired t -test was applied to evaluate if the mean difference between the amounts of calcium adsorbed to each mineral in the presence of nitrate and sulfate, respectively, differed from zero at $P = 0.05$. Calculations were performed using SAS software, version 9.3 [30].

The electrokinetic experiments involved at least 10 runs per sample. From this the averaged electrophoretic mobility was used, and the standard error was noted as specified by the software.

The second harmonic generation experiments allow clear observation of equilibrium states as well. As for the electrokinetic experiments, transient effects were absent when the reported data points were collected. The data were scaled to the signal in pure water, which was measured before and after a concentration series. The temperature dependence was studied with a setup that was previously used in ice-nucleation studies.

3. Results and discussion

3.1 Mineral characterization

The XRD patterns (**Figure 1**) show some accessory quartz with kaolinite and no other phase with gibbsite [31]. The plate-shaped morphologies of the mineral particles conform to the pseudo-hexagonal plates of kaolinite [32] and the plate-like lozenges or plate-like gibbsite hexagons [33] (**Figure 2**).

The specific surface area of the kaolinite sample ($30.9 \text{ m}^2 \text{ g}^{-1}$) is within the interval from 5 to $39 \text{ m}^2 \text{ g}^{-1}$ reported for this mineral [34]. The gibbsite surface area ($26.6 \text{ m}^2 \text{ g}^{-1}$) is close to that calculated by Rosenqvist and Casey [35] from the density and particle dimensions of a gibbsite sample prepared using the same

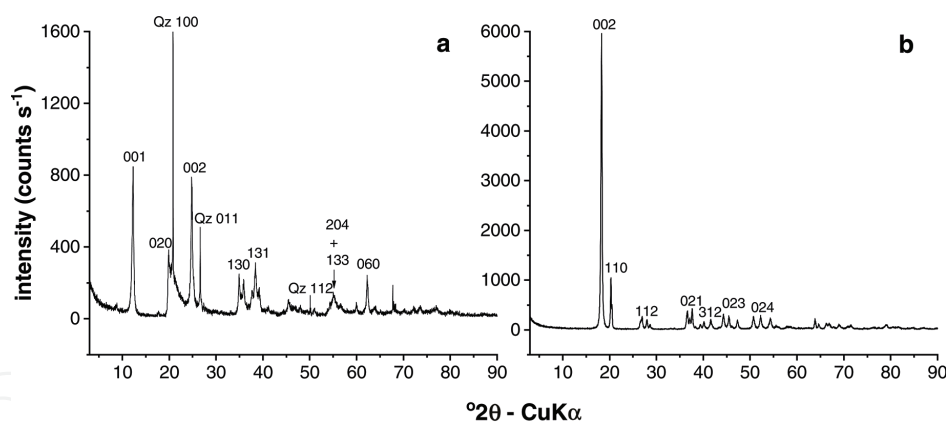


Figure 1. X-ray diffraction patterns of (a) kaolinite and (b) gibbsite samples. Qz = quartz.

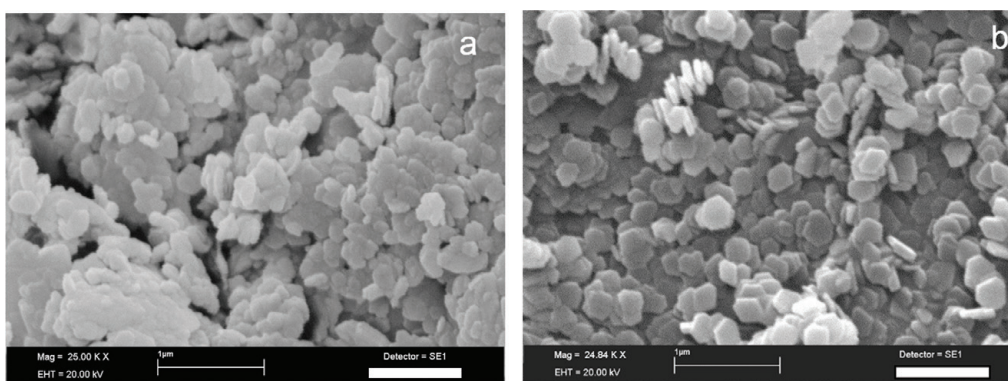


Figure 2. Scanning electron micrographs of (a) kaolinite and (b) gibbsite samples.

procedure followed here ($25 \text{ m}^2 \text{ g}^{-1}$). However, their reported N_2 -BET surface area is somewhat lower ($19.6 \text{ m}^2 \text{ g}^{-1}$).

The respective IEP values found for kaolinite and gibbsite are 4.9 and 10.6 (**Figure 3**). The kaolinite IEP is close to the value compiled by Stumm and Morgan [36] (4.6). The gibbsite one is in between the pristine point of zero charge at pH 10.0 found by Hiemstra et al. [26] and the IEP at pH 11.3 reported by Adekola et al. [37] for gibbsites with surface areas above $25 \text{ m}^2 \text{ g}^{-1}$.

3.2 Calcium adsorption on kaolinite

The batch experiments were carried out without attempting to exclude CO_2 . In principle, calcite bulk precipitation could also decrease the equilibrium aqueous calcium concentrations. However, according to equilibrium calculations, the pH threshold value needed for calcite formation in the 10-mM calcium solutions in the absence of calcium adsorption is about 7.7. Considering that this pH value increases as the initial calcium concentration in solution decreases, calcite formation in our mineral suspensions can be safely excluded because the highest equilibrium pH was 6.9. Furthermore, we assumed that the aqueous bicarbonate (HCO_3^-) ($\sim 2.4 \text{ } \mu\text{M}$ as calculated with Visual MINTEQ) did not affect the sulfate adsorption. Helyar et al. [38] have found that 0.58 mM HCO_3^- did not influence phosphate adsorption on a gibbsite sample.

The amounts of calcium adsorbed to kaolinite from the dilute and concentrated solutions are presented in **Table 2**. The results for the dilute solutions (0.5 mM) with initial pH 4 showed that higher sulfate adsorption on kaolinite at low pH [16] did not enhance calcium adsorption via potential co-adsorption. This finding

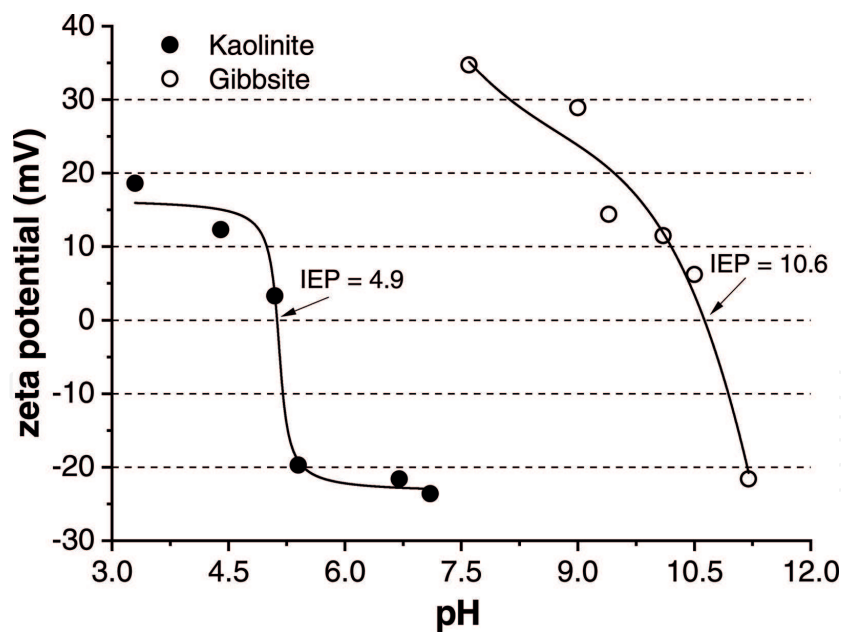


Figure 3.
Zeta potential values measured in kaolinite and gibbsite 0.01-M KNO₃ suspensions at different pH conditions. IEP = isoelectric point.

Solution	pH		Ca ²⁺	
	Initial	Equilibrium	μmol m ⁻²	(%) ^a
0.5 mM Ca(NO ₃) ₂ ·4H ₂ O	4.0	4.2	0.0a	00.0a
0.5 mM CaSO ₄ ·2H ₂ O	4.0	4.4	0.0a	00.0a
0.5 mM Ca(NO ₃) ₂ ·4H ₂ O	6.0	5.1	0.4 <i>b</i>	21.7 <i>b</i>
0.5 mM CaSO ₄ ·2H ₂ O	6.0	5.2	0.4 <i>b</i>	22.7 <i>b</i>
10 mM Ca(NO ₃) ₂ ·4H ₂ O	4.0	4.0	3.2A	09.4A
10 mM CaSO ₄ ·2H ₂ O	4.0	4.1	1.6B	05.3B
10 mM Ca(NO ₃) ₂ ·4H ₂ O	6.0	4.7	1.6A	05.1A
10 mM CaSO ₄ ·2H ₂ O	6.0	4.9	0.8B	02.6B

^aCalculated in relation to the initial calcium concentration.
Means followed by the same letter in the same column do not differ at P = 0.05 according to the paired t-test. Lowercase letters refer to comparisons of dilute solutions (0.5 mM); uppercase letters refer to comparisons of concentrated solutions (10 mM).
Normal letters refer to comparisons between solutions at initial pH 4; italicized letters refer to comparisons between solutions at initial pH 6.

Table 2.
Initial and equilibrium pH values and amounts of calcium adsorbed on kaolinite in the presence of nitrate and sulfate.

suggests that a possible increase in negative surface charges following from sulfate adsorption was insufficient to overcome the electrostatic repulsion to calcium ions exerted by positive surface charges. In this case, positive charges superseded negative ones because the equilibrium pH values remained below the kaolinite IEP. These results also indicate that even starting to deprotonate at pH 3 [39], the silanol surface groups of kaolinite did not adsorb calcium. The local electrostatic repulsion from the positively charged aluminol surface groups of kaolinite, which deprotonate above pH 8.7 [39], may have outweighed the attraction exerted by the negatively charged silanol groups on calcium at low pH and low ionic strength. Calcium adsorption to kaolinite from the 0.5-mM solutions with initial pH 6 was

the same in the presence of either nitrate or sulfate. Therefore, no sulfate-calcium co-adsorption occurred under the net negative surface charge condition provided by equilibrium pH values (5.1 and 5.2) higher than the kaolinite IEP (4.9).

The increase in the initial concentration of calcium sulfate (10 mM) reduced calcium adsorption on kaolinite by 50% relative to those measured in the presence of 20 mmol_c L⁻¹ of nitrate for the two initial pH conditions. Equilibrium calculations (**Table 1**) indicate that the neutral pair CaSO₄⁰ comprises 31% of the total calcium dissolved in the 10 mM calcium sulfate solution for both pH values, which decreases free calcium ion activity in the sulfate solutions to about 63% of those calculated for the nitrate solutions. The enhanced formation of neutral ion pairs containing an adsorptive and/or lowering the activity of its ionic free form in solution may decrease its adsorption [23, 40] and outweigh potential co-adsorption. Furthermore, the reduction of Ca²⁺ and SO₄²⁻ activities in solution due to adsorption did not seem to promote an appreciable shift in the equilibrium of CaSO₄⁰ formation toward free aqueous Ca²⁺ and SO₄²⁻, which could lead to comparable conditions of free ions in the nitrate solutions. Finally, unlike the observed for the dilute solutions presenting initial pH 4, the enhancement of calcium loading to 10 mM resulted in calcium adsorption on kaolinite overcoming the electrostatic repulsion from the net positive surface charge of that mineral at equilibrium.

3.3 Calcium adsorption on gibbsite

The amounts of calcium adsorbed on gibbsite from all solutions are presented in **Table 3**. Although according to Eqs. (1) and (2) sulfate adsorption to gibbsite could favor sulfate-calcium coadsorption, such a trend was not observed for the dilute and acidic conditions (0.5 mM; pH 4). At equilibrium pH ~ 7, calcium adsorption on gibbsite from the dilute solutions only occurred in the presence of sulfate. Because of the high IEP of the studied gibbsite, all adsorption experiments corresponded to a net positive surface charge. Sulfate adsorption and pH enhancement reduce the positive charges and concomitant electrostatic repulsion of calcium. Therefore,

Solution	pH		Ca ²⁺	
	Initial	Equilibrium	μmol m ⁻²	(%) ^a
0.5 mM Ca(NO ₃) ₂ ·4H ₂ O	4.0	4.3	0.0a	0.0a
0.5 mM CaSO ₄ ·2H ₂ O	4.0	4.5	0.0a	0.0a
0.5 mM Ca(NO ₃) ₂ ·4H ₂ O	6.0	6.5	0.0a	0.0a
0.5 mM CaSO ₄ ·2H ₂ O	6.0	6.9	0.2b	8.2b
10 mM Ca(NO ₃) ₂ ·4H ₂ O	4.0	4.4	1.9A	4.3A
10 mM CaSO ₄ ·2H ₂ O	4.0	4.6	0.9B	2.6B
10 mM Ca(NO ₃) ₂ ·4H ₂ O	6.0	6.2	0.0A	0.0A
10 mM CaSO ₄ ·2H ₂ O	6.0	6.8	0.0B	0.0B

^aCalculated in relation to the initial calcium concentration.

Means followed by the same letter in the same column do not differ at P = 0.05 according to the paired t-test. Lowercase letters refer to comparisons of dilute solutions (0.5 mM); uppercase letters refer to comparisons of concentrated solutions (10 mM).

Normal letters refer to comparisons between solutions at initial pH 4; italicized letters refer to comparisons between solutions at initial pH 6.

Table 3.
Initial and equilibrium pH values and amounts of calcium adsorbed on gibbsite in the presence of nitrate and sulfate.

our results suggest that besides sulfate adsorption, the net positive surface charge, which also depends on solution pH and ionic strength, affected calcium sulfate co-adsorption on gibbsite. Sulfate also decreased calcium adsorption on gibbsite from the more concentrated acidic solutions (10 mM; pH = 4), presumably due to the same mechanisms as those proposed for kaolinite.

4. pH and salt concentration effects on calcium adsorption on kaolinite and gibbsite

Unlike the enhancing pH effect on calcium adsorption on kaolinite observed for the 0.5-mM solutions containing either nitrate or sulfate, an opposite effect was found for the two more concentrated solutions (10 mM) containing those anions. In these cases, an initial pH increase from 4 to 6 decreased absolute calcium adsorption by 50% on kaolinite and by 100% on gibbsite.

This negative pH effect on calcium adsorption from the 10-mM solutions can be considered analogous to the positive pH effect on orthophosphate adsorption on kaolinite observed in previous papers for acidic condition (pH < 7) [41–43]. Such an effect concurs with negative charge enhancement on the kaolinite surface, which disfavors orthophosphate adsorption. On the other hand, the orthophosphate adsorption to kaolinite from dilute solutions decreases as solution pH increases, which resembles the P adsorption behavior of iron oxides [44]. He et al. [45] suggested that the aqueous P speciation may be related to the positive pH effect on orthophosphate adsorption to kaolinite. However, such an association does not seem plausible: according to equilibrium calculations based on NIST 46.7 stability constant database, the aqueous orthophosphate species (H_2PO_4^-) prevails from pH ranging from 3 to 7. Likewise, for pH ranging from 4 to 7, calcium speciation in the studied 10-mM solutions does not differ from results in **Table 1**. Therefore, higher salt concentration should be associated with low calcium adsorption at higher pH values. This hypothesis will be discussed below.

While the basal planes of kaolinite have been considered to hold permanent negative charges [46], recent surface force measurements carried out with atomic force microscopes have shown that the surface charges of the silica basal plane of kaolinite and the alumina basal plane of kaolinite and gibbsite react to changes in solution pH and salt concentration as the variable charges found on edge faces of those minerals [19–21]. Furthermore, the solution effects on basal silica surface charges differ from those observed for alumina faces [19, 21], and even for a given basal plane, the magnitudes of the surface charges can change when the dissolved cation constitutes the sole difference among the solutions in contact with the mineral [20].

Such complex, anisotropic charge behavior may be relevant to our findings given the apparent unexpected negative pH effect on calcium adsorption. Weak calcium hydrolysis suggests that uptake on oxide-like surface groups, such as those on kaolinite and gibbsite edges, only occurs at relatively high pH [15, 47]. Therefore, the basal planes of kaolinite and gibbsite may be the main adsorption sites of that cation at pH < 7 [19, 21]. Although Siretanu et al. [20] observed calcium adsorption from CaCl_2 solutions at pH 6 for the alumina face of nanosized gibbsite, their surface force measurements indicated that calcium adsorption from solutions with increasing concentrations of that cation initially increased followed by a decrease in the extracted charge densities with a maximum between 5 and 10 mM CaCl_2 . The authors argued that the concurrent increasing co-adsorption of chloride ions could explain the decrease in surface force. Unfortunately, the amounts of adsorbed calcium cannot be assessed in such experiments as from batch adsorption studies. On

the other hand, batch adsorption results cannot be associated with a given surface plane. The maximum diffuse layer potential from force measurements can likewise be explicated by constant or increasing calcium adsorption overcompensated by screening due to chloride adsorption in the Stern layer or simple double-layer screening.

In our experiments with the 10-mM solutions, the mean potential differences across the electrical double layer of gibbsite at equilibrium, as estimated by the Nernst Equation [48], were + 360 and + 242 mV for the more and less acidic solutions, respectively. These values, which are upper limit estimates, indicate that anion adsorption should be disfavored in the less acidic suspension. In the kaolinite scenarios with the 10-mM solutions, the mean Nernst surface potentials were also positive at equilibrium, i.e., +50 and + 5.6 mV for more and less acidic solutions, respectively. The lower values compared to those calculated for gibbsite, and a possible difference between the screening effects on silica and alumina basal planes, could cause a moderate reduction in calcium adsorption on kaolinite from the less acidic nitrate and sulfate solutions. For the experiments with the dilute solutions (0.5 mM), the low salt concentration was insufficient for promoting appreciable screening effects.

4.1 Electrokinetic measurements

Figure 4 displays the results of electrokinetic measurements carried out for kaolinite and gibbsite suspensions at pH 5. In general, the electrokinetic mobility (EM) values measured against increasing salt concentrations showed the same trends for both studied minerals. The increasing sulfate addition as Na_2SO_4 enhanced the negative surface charge of both kaolinite and gibbsite (**Figure 4(a)**). However, in the gibbsite scenario, sulfate caused charge reversal at the concentration of about 0.3 mM Na_2SO_4 . Data obtained via the increasing addition of CaCl_2 to kaolinite and gibbsite in the presence of 3 mM Na_2SO_4 demonstrated rather a shielding effect, mainly for the gibbsite scenario where no clear charge reversal was observed at 3 mM Ca^{2+} (**Figure 4(b)**). In a mixed CaSO_4 system up to the solubility limit, we retrieved the sulfate effect of increasing the surface negative charge (**Figure 4(c)**). Electrophoretic mobility measurements are usually unstable when performed at pH value close to the mineral IEP; such an instability probably resulted in EM values somewhat different for kaolinite in the absence of Na_2SO_4 (**Figure 4(a)**) and CaSO_4 (**Figure 4(c)**). Despite this, the obtained results corroborate the idea that co-adsorption of calcium due to sulfate adsorption is a minor feature.

4.2 Surface charge modeling applied to gibbsite

Some of our assumptions also agree with gibbsite surface charge trends simulated with the diffuse layer model (DLM) [49] using the calcium/gibbsite and sulfate/gibbsite surface complexation constants available in [15] as well as Eqs. (1)–(3). The simulations were performed for standard gibbsite suspensions (10 g L^{-1}) in solutions containing dual cation-anion combinations with sodium, calcium, nitrate, and sulfate, where nitrate and sodium ions do not interact with the surfaces via chemical reactions. Binary systems were chosen as references of both inert ions (sodium and nitrate) and their mixtures with sulfate and calcium. Although the standard gibbsite as treated by Karamalidis and Dzombak [15] has an IEP of 9 (i.e., lower than in the present case), the calculation results illuminate calcium adsorption in the mixed system. Unfortunately, self-consistent data for a more complex surface complexation model are not available. The authors are well

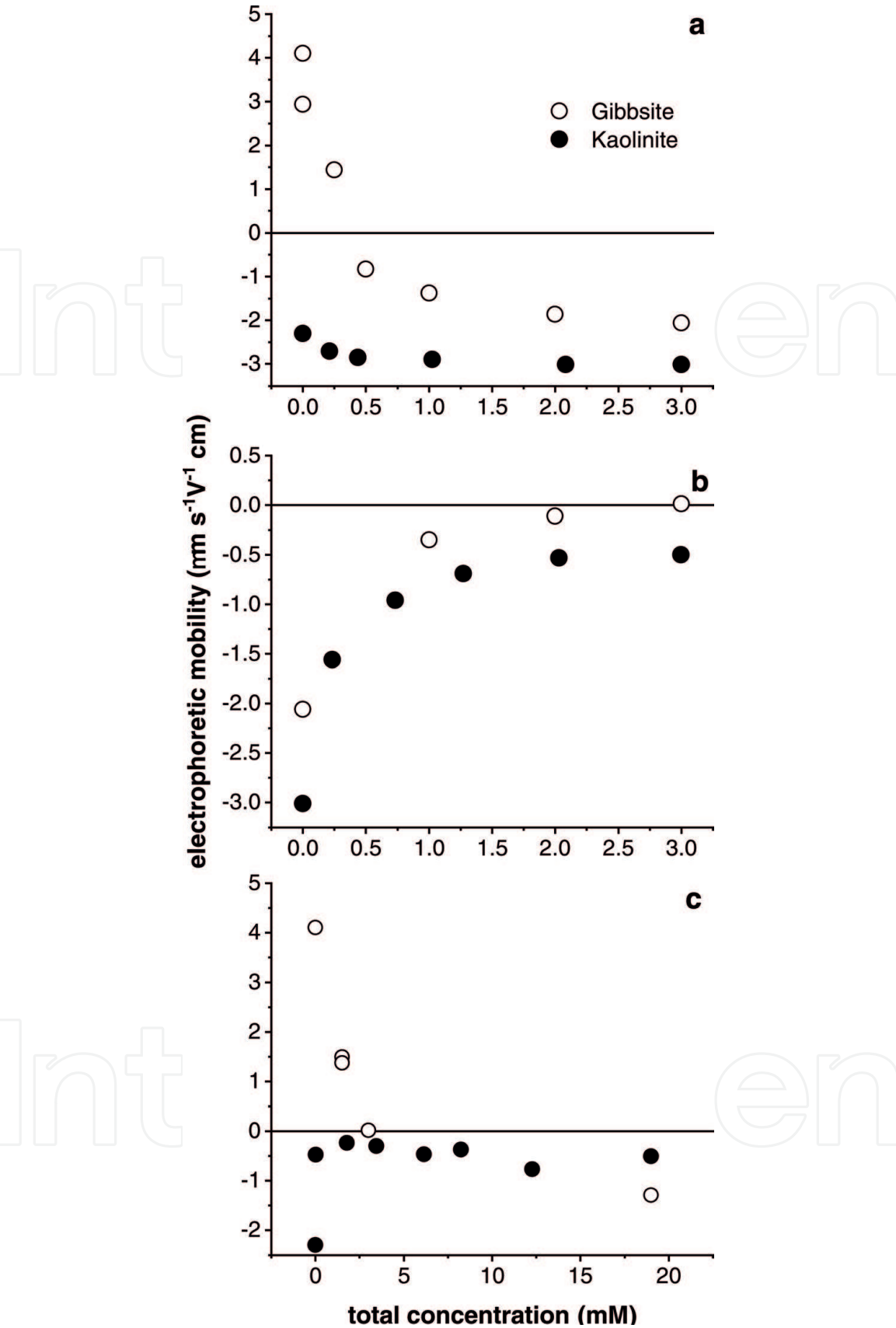


Figure 4.
Electrophoretic mobility values of kaolinite and gibbsite suspensions measured under increasing concentrations of (a) Na₂SO₄, (b) CaCl₂ + 3 mM Na₂SO₄, and (c) CaSO₄.

aware about the drawback of using a simple DLM. With the available data, it was not possible to design a separate model. The present modeling, for example, disregards the available information about the nature of the surface complexes (inner sphere vs. outer sphere) or the calcium adsorption on the basal planes, because the

DLM only includes inner-sphere surface complexes and the model does not distinguish crystal planes. Also when the data base was generated, the information about the Ca adsorption at low pH had not been available. Furthermore, in the following the comparisons between solutions containing 1:1, 2:1 and 2:2 electrolyte solutions are difficult to directly compare, since at the same time the ionic strength and the cation concentrations might be changing for a given concentration of the electrolyte (this is also true for the subsequent sections).

The enhancement of an inert electrolyte concentration increases the gibbsite charge at a fixed pH with no shift in the IEP (**Figure 5(a)**). The diffuse layer model in the database used for the calculations causes a steep charge increase due to the absence of a Stern layer. This behavior is hidden when plotting titration raw data (i.e., total acid and base added versus pH). As depicted in **Figure 5(b)**, calcium does not significantly affect the curves relative to **Figure 5(a)**. The charge for a given cation concentration and pH increases because the negative counterion concentration is higher in the calcium presence, allowing for better shielding and increased charge. The enhanced charge is not due to calcium adsorption, which is insignificant.

Figure 5(c) shows two effects relative to the gibbsite surface charge as a function of sodium sulfate concentration. One is sulfate uptake, which greatly decreases surface charge density. For the two lowest sulfate concentrations, all sulfate is adsorbed with nearly no negatively charged counterion to shield positive charges, thereby limiting the number of positively charged surface groups. The situation changes for the high-sulfate concentration: first, the IEP is decreased due to adsorbed sulfate. Less than 15% sulfate is adsorbed at the lowest pH, leaving a substantial negative charge to allow the increase in protonated surface groups as pH decreases. Calcium sulfate (**Figure 5(d)**) behaves similarly to sodium sulfate; according to the model, calcium adsorption does not occur at low pH. The formation of the CaSO_4^0 ion pair in solution affects ionic strength and free sulfate activity; hence the charge is higher in the sodium sulfate system. The model does not predict enhanced calcium uptake and indicates that no system charge reversal occurred at the pH values investigated experimentally. Even so, a possible relative increase in neutral aluminol groups ($\equiv\text{AlOH}^0$) at pH ~ 7 occurred in our experiments to favor the sulfate-calcium co-adsorption on gibbsite from the 0.5 mM CaSO_4 solution.

4.3 Considerations from kaolinite titration data

Riese [50] titrated kaolinite in CaCl_2 , NaNO_3 , and Na_2SO_4 solutions, and we show the resulting curves in **Figure 6**. The results for NaNO_3 (**Figure 6(a)**) showed a typical trend with increasing salt concentration, i.e., a higher titrable charge in a higher electrolyte solution. The absence of spread as a function of salt level observed at low Na_2SO_4 concentrations (**Figure 6(b)**) could indicate sulfate adsorption when related to the calculations for gibbsite (**Figure 5(c)**). However, for the previous gibbsite charge simulations, the total charge was assessed, whereas for kaolinite the titrable one was determined. The titration data in CaCl_2 showed a very small spread and surprisingly low values for the titrable charge as compared to NaNO_3 (**Figure 6(c)**) perhaps because the interaction of calcium with the kaolinite surface hindered proton release. Such an interaction would not apply to the kaolinite edge; also, oxidic surface functional groups on edge faces are not expected to bind to calcium at low pH values. Thus, the interaction is more likely with basal planes. Kumar et al. [21] found similar features on the kaolinite gibbsite face and reported visible co-adsorption of chloride at 100 mM CaCl_2 concentration. The influence of calcium adsorption on basal surfaces on proton release must be studied to understand the systems. Clearly, the available data suggest that both sulfate and

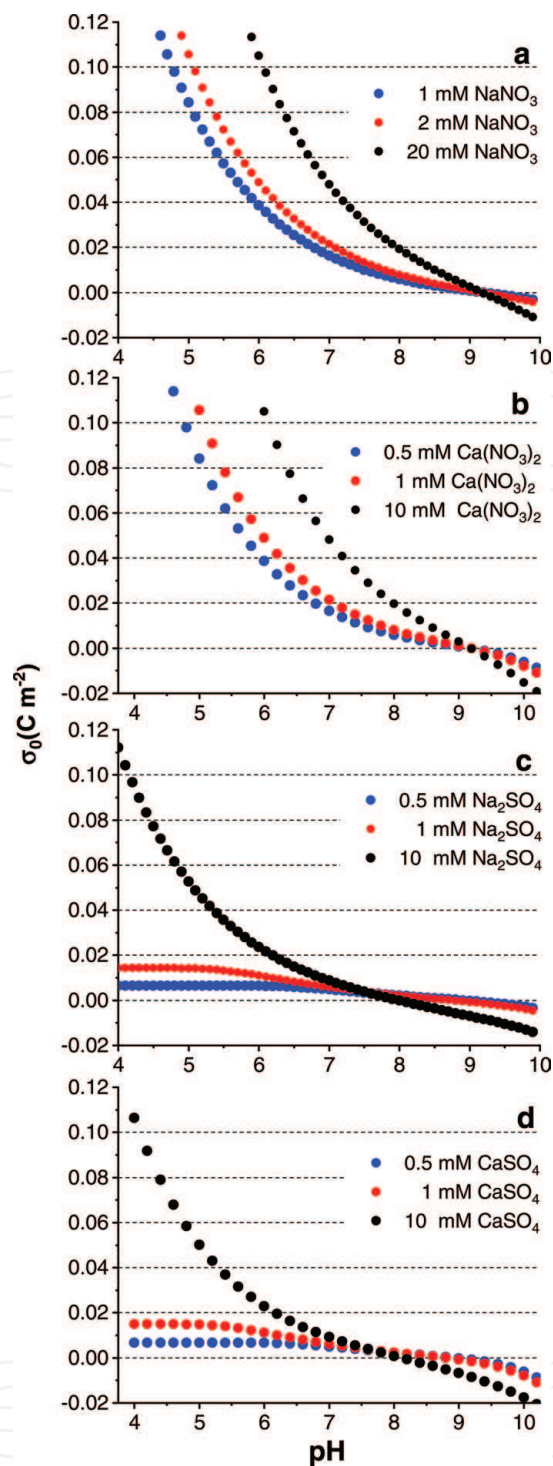


Figure 5. Net surface charge (σ_0) values calculated using the double layer model for standard gibbsite in 10-g L^{-1} aqueous suspensions as a function of pH, salt concentration, and composition: (a) NaNO_3 , (b) $\text{Ca}(\text{NO}_3)_2$, (c) Na_2SO_4 , and (d) CaSO_4 .

calcium each interact with kaolinite at pH 4 and 6, rendering cooperative interactions possible; this trend supports experimental data from our CaSO_4 systems.

4.4 Second harmonic generation experiments at room temperature

Figure 7 shows results of second harmonic generation (SHG) experiments at pH 6 with the c-cut of sapphire. The setup has been described in much detail before [28, 29]. As pointed out before, this crystal plane is more or less structurally equivalent to the gibbsite basal plane, which is present on both gibbsite and kaolinite. Numerous investigations have shown that this plane has a low isoelectric point.

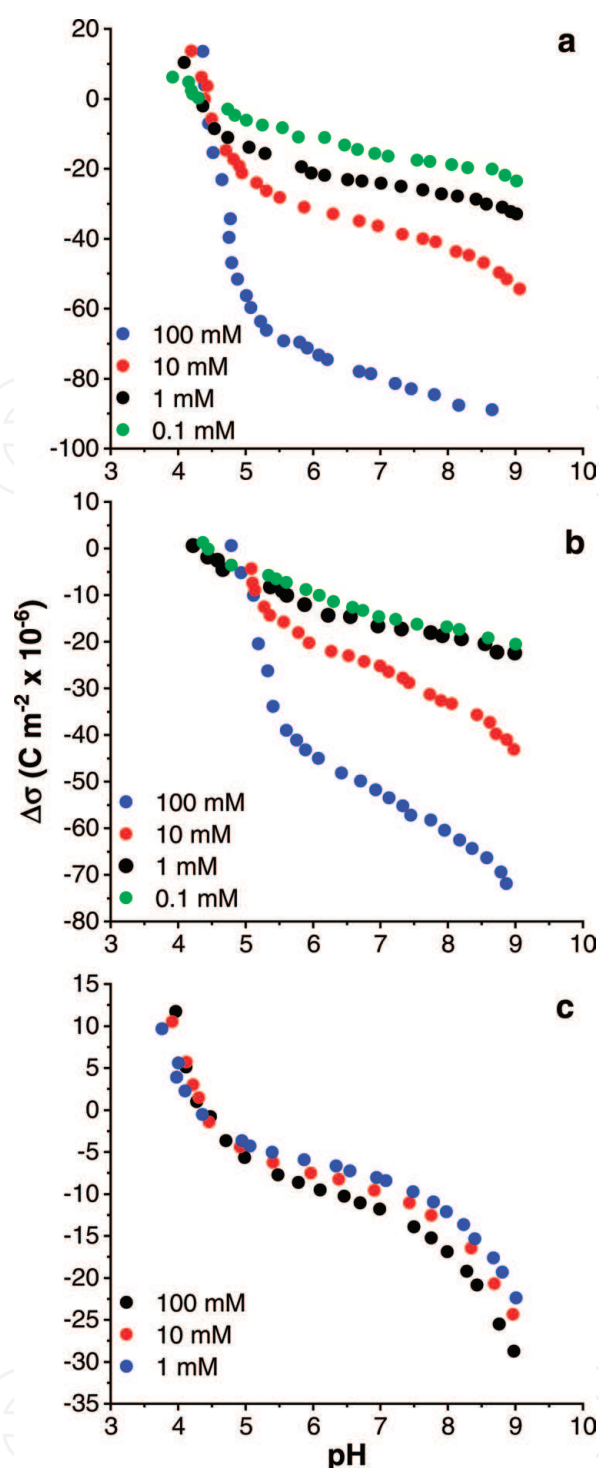


Figure 6. Titrable surface charge ($\Delta\sigma$) values obtained by Riese [50] for kaolinite KGa-1 suspended in solutions of (a) NaNO_3 , (b) Na_2SO_4 , and (c) CaCl_2 .

So it is probable that at pH 6, the surface is negatively charged. **Figure 7(a)** shows the results for Na_2SO_4 addition that correspond to those shown in **Figure 4(a)**. The experiment is started from a water solution to which Na_2SO_4 is added, and the signal is referenced to the signal in water (this is also the case for all the other data in **Figure 7**). The increase in the SHG signal indicates less positive or more negative charge. Assuming that the sapphire surface is negative at this pH value, it would mean more negative charge and correspond to data on kaolinite rather than those on gibbsite. Also the change in signal is quite small, which also is the case for kaolinite in **Figure 4(a)**. The unexpected adsorption of anions on the negatively charged basal plane of sapphire has also been reported by others. Starting from a solution containing about 1.5 mM sulfate, the addition of CaCl_2 results in a much

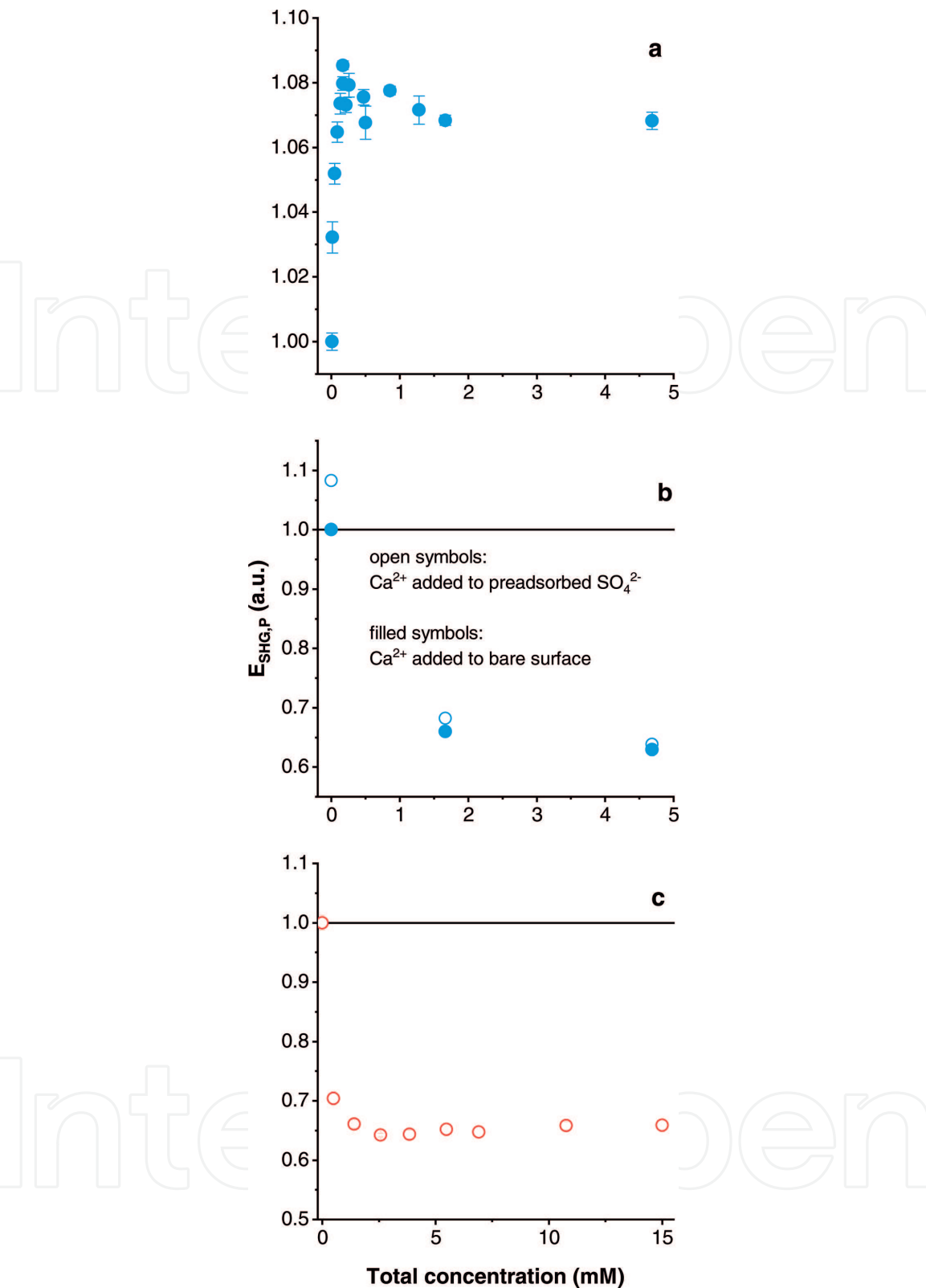


Figure 7. Second harmonic generation electric field of sapphire basal planes measured under increasing concentrations of (a) Na_2SO_4 , (b) $CaCl_2 + 1.5\text{ mM } Na_2SO_4$, and (c) $CaSO_4$.

stronger change in the signal (**Figure 7(b)**). This is the same as what was observed in **Figure 4(b)** for both gibbsite and kaolinite. The SHG results on the basal plane clearly mimic the electrokinetic behavior. Furthermore, addition of $CaCl_2$ to the bare surface shows the same behavior irrespective of the absence and presence of sulfate as can be seen in **Figure 7(b)**. This would suggest that the divalent cation is strongly shielding the negative charge, whereas it is not clear whether charge reversal occurs. The SHG data cannot indicate charge reversal. The electrokinetic data

for gibbsite might suggest charge reversal at higher Ca concentrations, which in turn would agree with the observation of Siretanu et al. [20] who directly observed the specific interaction of Ca with gibbsite basal planes. As for **Figure 7(a)**, the results for the basal plane from **Figure 7(b)** concur with the data for the particles from **Figure 4(b)**, which could suggest the relevance of the basal planes in the reactions of the particles. Finally in **Figure 7(c)**, CaSO_4 solutions have been added to the sapphire basal plane to mimic the results from **Figure 4(c)**. Similar to the discussion with respect to **Figures 4(a)** and **7(a)**, it appears that the SHG is more comparable to the kaolinite system, since the decrease of the signal is rather showing either an increase in positive charge or a decrease in negative charge. The latter happens in **Figure 4(a)** for kaolinite, but none of the options would be applicable for gibbsite. Also the strong change at the lower concentration and the quick plateauing occurs for the kaolinite (**Figure 4(c)**) and for the sapphire basal plane (**Figure 7(c)**). While this cannot exclude a role played by sulfate that is very apparent for gibbsite (**Figure 4(c)**), the predominant role of calcium is obvious. So the role of the calcium sulfate ion pair remains elusive also based on these results, while the small but discernible increase in the signal in the CaSO_4 system indicates sulfate interaction at concentrations above 5 mM (**Figure 7(c)**).

To further investigate the role of these ion pairs, temperature-dependent experiments were carried out. The results will be presented and discussed in the final section.

4.5 Second harmonic generation experiments at variable temperature

Preliminary speciation calculations using various data bases were performed to gain knowledge about the extent of ion-pair formation when the temperature is changed. Calculations were done for 15 mM solutions of divalent ions, starting from 20°C. **Figure 8(a)** shows that with decreasing temperature the extent of ion-pair formation decreases (for CaCl_2) or remains approximately constant (for Na_2SO_4). For both systems the dominant ion pairs make up less than 10%. This is different for the CaSO_4 system, where (as could be expected) a decrease in the extent of ion-pair formation occurs with decreasing temperature. Clearly also the ion pair makes up more than 30% as discussed in previous sections. The concomitant solutions were put into contact with sapphire basal planes and studied as a function of temperature by second harmonic generation. The setup used in this case has been extensively described [28, 29]. **Figure 8(b)** shows results of second harmonic generation (SHG) experiments, starting with 15 mM solutions of the divalent ions at pH 6 and room temperature with decreasing temperature. In water the SHG signal is changing little. This is similar for the sodium sulfate system, which is also similar to water. In agreement with the results shown in **Figure 7(a)**, where only small changes were observed in that system. Actually data not shown for about 15 mM sulfate showed on average 1.06 times the water signal. With the average water signal at 0.535 at 20°C, we obtain a value of 0.567 in the presence of 15 mM sulfate, which is within the range of signals collected in the temperature dependence curve. The black curve also suggests a slight decrease of the signal for the sulfate signal compared to water at 4°C, but even here the scatter remains too large to draw ultimate conclusions. With decreasing temperature the sulfate adsorption should increase, but with respect to **Figure 7**, it was concluded that Ca was the more important ion in this system. The more interesting systems in this temperature range in the SHG experiments with the c-cut of sapphire are clearly also the Ca systems. The quite strong decrease in the signal for both Ca systems is observed. The stronger extent in CaCl_2 solutions at 15 mM is also observed (giving 0.6 of the water signal, data now shown). Most interestingly, a trend with temperature occurs in the chloride system

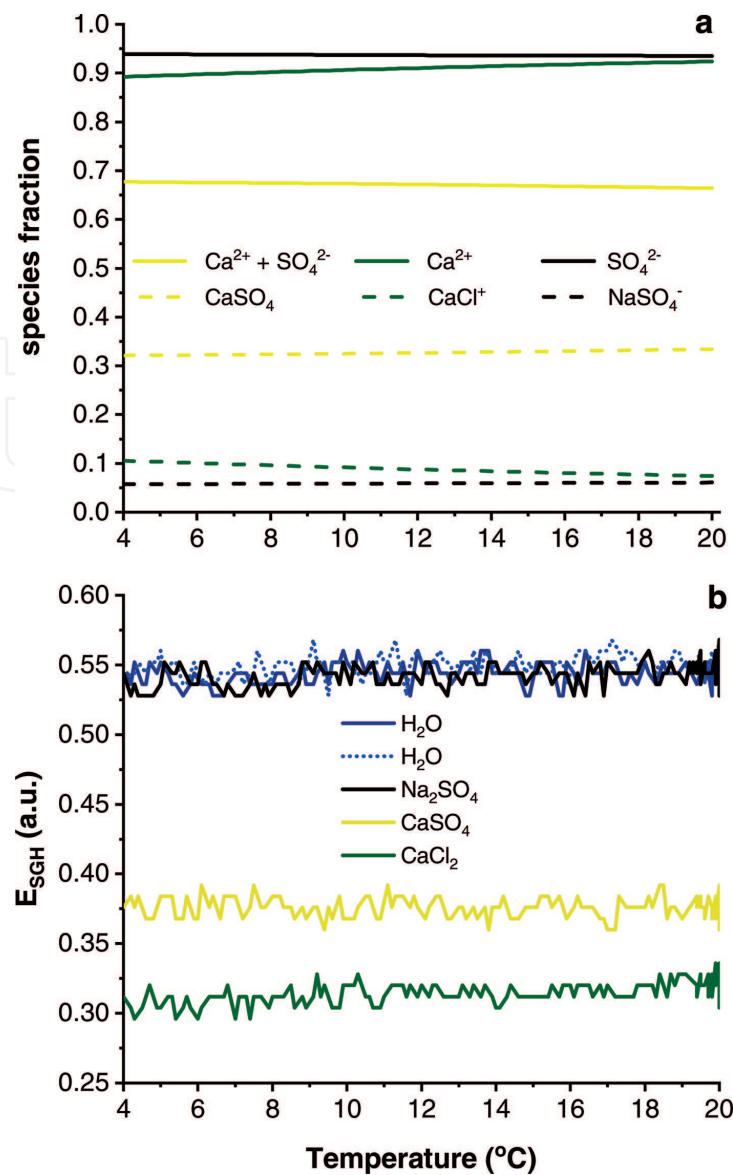


Figure 8. Comparison of Na_2SO_4 (black) CaCl_2 (green) CaSO_4 (yellow) solutions (15 mM of divalent ions at 20 °C) between 4 and 20 °C with respect to speciation (a) and second harmonic signal (b). (b) also includes two runs with water only, one before and one after the experiments with the salt solutions.

to lower signal with lower temperature, while the CaSO_4 system remains constant. If a decrease in the signal is associated with stronger positive charge, it would suggest that there is a role of sulfate in the CaSO_4 system, which may be triggered by the decreased ion-pair formation, making more sulfate available with decreasing temperature. Note that overall much more free Ca is available in the CaCl_2 system, even if it is slightly decreasing with decreasing temperature. So decreasing temperature would favor at the same time enhanced sulfate interaction (anions adsorb more strongly on oxides with decreasing temperature) and make more free ions available, which would also favor uptake. Based on the results, the effects of temperature on sulfate would then outcompete those on calcium, but the role of the ion-pair formation could become visible. More experiments with different concentrations would be helpful in gaining more insight. Additional experiments with more soluble MgSO_4 are also planned. The formation of the ion pairs can also be an issue in freezing processes on surfaces in the presence of ions like Ca and sulfate, which can be expected in aerosols due to their presence in sea water. This could be an interesting link between the aqueous chemistry and the atmospheric chemistry which has not been explored to the extent possible.

5. Conclusions

The findings of this chapter, which are associated to acidity conditions ranging from an unsuitable to a more favorable one for cropping, indicate that sulfate adsorption has no or little positive effect on calcium adsorption on kaolinite and gibbsite. On the other hand, as both calcium and sulfate concentrations in the solution phase are increased toward the precipitation threshold of calcium sulfate, calcium adsorption on those minerals is inhibited. Further, for a higher initial calcium loading (10 mM), the equilibrium pH enhance from 4.0 to 6.9 decreases calcium adsorption to kaolinite and gibbsite. Besides indicating low calcium adsorption on gibbsite, the experimental data suggest that the application of higher amounts of sulfate-concentrated products such as gypsum on lime-amended oxisols tends to reduce the effectiveness of kaolinite, the main clay-sized mineral responsible for the cation exchange capacity of those soils, to impair calcium leaching. The results also suggest that hematite and goethite are the main oxisol clay-sized minerals responsible for the calcium sulfate co-adsorption reported to oxisol samples. This hypothesis should be evaluated in future research. From the data presented in this chapter, it seems that sulfate at the pH conditions considered dominates the gibbsite behavior, while on kaolinite the calcium is the more relevant ion. The basal plane of sapphire as studied with second harmonic generation yields results that are in close agreement with those of the kaolinite particles, which suggests that the kaolinite behavior might be explained by its gibbsite plane. The role of the ion pair in solution and of sulfate even on negatively charge surfaces has been discussed, and the relevance of studying these features also with respect to atmospheric sciences (freezing of water and ice nucleation on particle surface) was addressed. In particular the link between aqueous chemistry and ice nucleation should be used to understand processes the atmosphere.

Author details

Ahmed Abdelmonem^{1*}, Yujun Wang², Johannes Lützenkirchen³
and Marcelo Eduardo Alves⁴

¹ Institute of Meteorology and Climate Research, Karlsruhe Institute of Technology, Karlsruhe, Germany


² Key Laboratory of Soil Environment and Pollution Remediation, Institute of Soil Science, Chinese Academy of Sciences, Nanjing, PR China

³ Institute for Nuclear Waste Disposal, Karlsruhe Institute of Technology, Karlsruhe, Germany

⁴ Departamento de Ciências Exatas, Escola Superior de Agricultura 'Luiz de Queiroz' – ESALQ/USP, Piracicaba, SP, Brasil

*Address all correspondence to: ahmed.abdelmonem@kit.edu

IntechOpen

© 2018 The Author(s). Licensee IntechOpen. This chapter is distributed under the terms of the Creative Commons Attribution License (<http://creativecommons.org/licenses/by/3.0>), which permits unrestricted use, distribution, and reproduction in any medium, provided the original work is properly cited. 

References

- [1] Van Raij B. Gesso na Agricultura. Campinas: Instituto Agronômico; 2008. p. 233
- [2] Pavan MA, Bingham FT, Pratt PF. Redistribution of exchangeable calcium, magnesium, and aluminum following lime or gypsum applications to a Brazilian oxisol. *Soil Science Society of America Journal*. 1984;**48**:33-38. DOI: 10.2136/sssaj1984.03615995004800010006x
- [3] Alva AK, Gascho GJ. Differential leaching of cations and sulfate in gypsum amended soils. *Communications in Soil Science and Plant Analysis*. 1991;**22**:1195-1206. DOI: 10.1080/00103629109368484
- [4] Fahrenhorst C, Botschek J, Skowronek A, Ferraz J. Application of gypsum and lime to increase cation adsorption of a Geric Ferralsol in the Brazilian Amazon region. *Journal of Plant Nutrition and Soil Science*. 1999;**162**:41-47. DOI: 10.1002/(SICI)1522-2624(199901)162:1<41::AID-JPLN41>3.0.CO;2-6
- [5] Ernani PR, Miquelluti DJ, Fontoura SMV, Kaminski J, Almeida JA. Downward movement of soil cations in highly weathered soils caused by addition of gypsum. *Communications in Soil Science and Plant Analysis*. 2006;**37**:571-586. DOI: 10.1080/00103620500449443
- [6] Pearson RG. Hard and soft acids and bases. *Journal of the American Chemical Society*. 1963;**85**:3533-3539. DOI: 10.1021/ja00905a001
- [7] Bolan NS, Syers JK, Sumner ME. Calcium-induced sulfate adsorption by soils. *Soil Science Society of America Journal*. 1993;**57**:691-696. DOI: 10.2136/sssaj1993.03615995005700030011x
- [8] Marcano-Martinez E, McBride MB. Calcium and sulfate retention by 2 Oxisols of the Brazilian cerrado. *Soil Science Society of America Journal*. 1989;**53**:63-69. DOI: 10.2136/sssaj1989.03615995005300010012x
- [9] Alva AK, Sumner ME, Miller WP. Reactions of gypsum or phosphogypsum in highly weathered acid subsoils. *Soil Science Society of America Journal*. 1990;**54**:993-998. DOI: 10.2136/sssaj1990.03615995005400040010x
- [10] Davis JG, Burgoa B. Interactive mechanisms of anion adsorption with calcium leaching and exchange. *Soil Science*. 1995;**160**:256-264. DOI: 10.1097/00010694-199510000-00004
- [11] Pearce RC, Sumner ME. Apparent salt sorption reactions in an unfertilized acid subsoil. *Soil Science Society of America Journal*. 1997;**61**:765-772. DOI: 10.2136/sssaj1997.03615995006100030009x
- [12] Cichota R, Vogeler I, Bolan NS, Clothier BE. Cation influence on sulfate leaching in allophanic soils. *Australian Journal of Soil Research*. 2007;**45**:49-54. DOI: 10.1071/SR06070
- [13] Cichota R, Vogeler I, Bolan NS, Clothier BE. Simultaneous adsorption of calcium and sulfate and its effect on their movement. *Soil Science Society of America Journal*. 2007;**71**:703-710. DOI: 10.2136/sssaj2006.0206
- [14] Okuma DM, Alves ME. Anion and mineralogical effects on K⁺, Ca²⁺, and Mg²⁺ leaching in oxisols. *Soil Science*. 2011;**176**:115-123. DOI: 10.1097/SS.0b013e31820efe4c
- [15] Karamalidis AK, Dzombak DA. *Surface Complexation Modeling: Gibbsite*. Hoboken: John Wiley & Sons Inc.; 2010. p. 294

- [16] Essington ME, Anderson RM. Competitive adsorption of 2-ketogluconate and inorganic ligands onto gibbsite and kaolinite. *Soil Science Society of America Journal*. 2008;**72**:595-604. DOI: 10.2136/sssaj2007.0190
- [17] Tiberg C, Sjostedt C, Persson I, Gustafsson JP. Phosphate effects on copper(II) and lead(II) sorption to ferrihydrite. *Geochimica et Cosmochimica Acta*. 2013;**120**:140-157. DOI: 10.1016/j.gca.2013.06.012
- [18] Tiberg C, Gustafsson JP. Phosphate effects on cadmium(II) sorption to ferrihydrite. *Journal of Colloid and Interface Science*. 2016;**471**:103-111. DOI: 10.1016/j.jcis.2016.03.016
- [19] Liu J, Sandaklie-Nikolova L, Wang XM, Miller JD. Surface force measurements at kaolinite edge surfaces using atomic force microscopy. *Journal of Colloid and Interface Science*. 2014;**420**:35-40. DOI: 10.1016/j.jcis.2013.12.053
- [20] Siretanu I, Ebeling D, Andersson MP, Stipp SLS, Philippe A, Stuart MC, et al. Direct observation of ionic structure at solid-liquid interfaces: A deep look into the Stern layer. *Scientific Reports*. 2014;**4**:4956. DOI: 10.1038/Srep04956
- [21] Kumar N, Andersson MP, Van den Ende D, Mugele F, Siretanu I. Probing the surface charge on the basal planes of kaolinite particles with high-resolution atomic force microscopy. *Langmuir*. 2017;**33**:14226-14237. DOI: 10.1021/acs.langmuir.7b03153
- [22] Stumm W, Hohl H, Dalang F. Interaction of metal-ions with hydrous oxide surfaces. *Croatica Chemica Acta*. 1976;**48**:491-504
- [23] Mattigod SV, Gibali AS, Page AL. Effect of ionic-strength and ion-pair formation on the adsorption of nickel by kaolinite. *Clays and Clay Minerals*. 1979;**27**:411-416. DOI: 10.1346/Ccmn.1979.0270603
- [24] Hayes KF, Leckie JO. Modeling ionic-strength effects on cation adsorption at hydrous oxide-solution interfaces. *Journal of Colloid and Interface Science*. 1987;**115**:564-572. DOI: 10.1016/0021-9797(87)90078-6
- [25] Alves ME, Omotoso O. Improving Rietveld-based clay mineralogic quantification of oxisols using Siroquant. *Soil Science Society of America Journal*. 2009;**73**:2191-2197. DOI: 10.2136/sssaj2008.0365
- [26] Hiemstra T, Yong H, Van Riemsdijk WH. Interfacial charging phenomena of aluminum (hydr)oxides. *Langmuir*. 1999;**15**:5942-5955. DOI: 10.1021/la981301d
- [27] Gustafsson JP. Visual MINTEQ. Version 3.1. Stockholm: KTH Royal Institute of Technology; 2018. Available at: <http://vminteq.lwr.kth.se>
- [28] Abdelmonem A, Lützenkirchen J, Leisner T. Probing ice-nucleation processes on the molecular level using second harmonic generation spectroscopy. *Atmospheric Measurement Techniques*. 2015;**8**:3519-3526. DOI: 10.5194/amt-8-3519-2015
- [29] Lützenkirchen J, Abdelmonem A, Weerasooriya R, Heberling F, Metz V, Marsac R. Adsorption of dissolved aluminum on sapphire-c and kaolinite: Implications for points of zero charge of clay minerals. *Geochemical Transactions*. 2014;**15**:9. DOI: 10.1186/1467-4866-15-9
- [30] Hatcher L, Stepanski EJ. A Step-By-Step Approach to Using the SAS System for Univariate and Multivariate Statistics. Cary: SAS Institute Inc.; 1994. p. 552

- [31] Besoain E. Mineralogía de Arcillas de Suelos. San José: IICA; 1985. p. 1205
- [32] White GN, Dixon JB. Kaolin-serpentine minerals. In: Dixon JB, Schulze DG, editors. Soil Mineralogy with Environmental Applications. Madison: Soil Science Society of America; 2002. pp. 389-414
- [33] Sweegers C, de Coninck HC, Meekes H, Van Enckevort WJP, Hiralal IDK, Rijkeboer A. Morphology, evolution and other characteristics of gibbsite crystals grown from pure and impure aqueous sodium aluminate solutions. *Journal of Crystal Growth*. 2001;**233**:567-582. DOI: 10.1016/S0022-0248(01)01615-3
- [34] Dixon JB. Kaolin and serpentine group minerals. In: Dixon JB, Weed SB, editors. Minerals in Soil Environments. Madison: Soil Science Society of America; 2002. pp. 467-525
- [35] Rosenqvist J, Casey WH. The flux of oxygen from the basal surface of gibbsite [α -Al(OH)₃] at equilibrium. *Geochimica et Cosmochimica Acta*. 2004;**68**:3547-3555. DOI: 10.1016/j.gca.2004.02.022
- [36] Stumm W, Morgan J. Aquatic Chemistry: An Introduction Emphasizing Chemical Equilibria in Natural Waters. 2nd ed. New York: Wiley-Interscience; 1981. p. 780
- [37] Adekola F, Fedoroff M, Geckeis H, Kupcik T, Lefevre G, Lützenkirchen J, et al. Characterization of acid-base properties of two gibbsite samples in the context of literature results. *Journal of Colloid and Interface Science*. 2011;**354**:306-317. DOI: 10.1016/j.jcis.2010.10.014
- [38] Helyar KR, Munns DN, Burau RG. Adsorption of phosphate by gibbsite. I. Effects of neutral chloride salts of calcium, magnesium, sodium, and potassium. *Journal of Soil Science*. 1976;**27**:307-314. DOI: 10.1111/j.1365-2389.1976.tb02001.x
- [39] Brady PV, Cygan RT, Nagy KL. Molecular controls on kaolinite surface charge. *Journal of Colloid and Interface Science*. 1996;**183**:356-364. DOI: 10.1006/jcis.1996.0557
- [40] Lützenkirchen J. Ionic strength effects on cation sorption to oxides: Macroscopic observations and their significance in microscopic interpretation. *Journal of Colloid and Interface Science*. 1997;**195**:149-155. DOI: 10.1006/jcis.1997.5160
- [41] Muljadi D, Posner AM, Quirk JP. Mechanism of phosphate adsorption by kaolinite gibbsite and pseudoboehmite. I. Isotherms and effect of pH on adsorption. *Journal of Soil Science*. 1966;**17**:212-228. DOI: 10.1111/j.1365-2389.1966.tb01467.x
- [42] Chen YSR, Butler JN, Stumm W. Adsorption of phosphate on alumina and kaolinite from dilute aqueous solutions. *Journal of Colloid and Interface Science*. 1973;**43**:421-436. DOI: 10.1016/0021-9797(73)90388-3
- [43] Manning BA, Goldberg S. Modeling arsenate competitive adsorption on kaolinite, montmorillonite and illite. *Clays and Clay Minerals*. 1996;**44**: 609-623. DOI: 10.1346/Ccmn.1996.0440504
- [44] Gérard F. Clay minerals, iron/aluminum oxides, and their contribution to phosphate sorption in soils—A myth revisited. *Geoderma*. 2016;**262**:213-226. DOI: 10.1016/j.geoderma.2015.08.036
- [45] He LM, Zelazny LW, Baligar VC, Ritchey KD, Martens DC. Ionic strength effects on sulfate and phosphate adsorption on γ -alumina and kaolinite: Triple-layer model. Soil Science Society

of America Journal. 1997;**61**:784-793.
DOI: 10.2136/sssaj1997.0361599500610
0030011x

[46] Bolland MDA, Posner AM, Quirk JP. pH-independent and pH-dependent surface-charges on kaolinite. *Clays and Clay Minerals*. 1980;**28**:412-418. DOI: 10.1346/Ccmn.1980.0280602

[47] Geckeis H, Lützenkirchen J, Polly R, Rabung T, Schmidt M. Mineral-water interface reactions of actinides. *Chemical Reviews*. 2013;**113**:1016-1062. DOI: 10.1021/cr300370h

[48] Van Raij B, Peech M. Electrochemical properties of some Oxisols and Alfisols of tropics. *Soil Science Society of America Proceedings*. 1972;**36**:587-593. DOI: 10.2136/sssaj1972.03615995003600040027x

[49] Dzombak DA, Morel FMM. *Surface Complexation Modeling: Hydrous Ferric Oxide*. Hoboken: John Wiley & Sons Inc.; 1990. p. 393

[50] Riese AC. Adsorption of radium and thorium onto quartz and kaolinite: A comparison of solution/surface equilibria models [thesis]. Bolder: Colorado School of Mines; 1982